J. Org. Chem. **2001,** *66,* 7757−7764 **7757**

Dendralene-Type TTF Vinylogs Containing a 1,3-Diselenole Ring

Ramiya R. Amaresh, Dezhong Liu, Tatyana Konovalova, M. V. Lakshmikantham,
Michael P. Cava,* and Lowell D. Kispert*

Chemistry Department, University of Alabama, P.O. Box 870336, Tuscaloosa, Alabama 35487-0336

mcava@bama.ua.edu

Received June 26, 2001

2-Diformylmethylene-1,3-diselenole was prepared and condensed with dithiolium phoshonium bromides and dithiolium phosphonates in the presence of base to give dendralene-type vinylogs of TTF bearing a 1,3-diselenole moiety. The electrochemistry of these dendrimers was studied. SEEPR measurements were also carried out. Calculations were carried out on the radical cations and correlated with the EPR values.

Introduction

The discovery of one-dimensional conductivity in a complex derived from TTF (**1**) and TCNQ (**2**) in 1973[1] provided the impetus for unabated international activity aimed at the modification of the donor moiety to achieve better conductivity properties, to understand the nature of structure−activity relationships. Some of these efforts involved the replacement of the sulfur atoms in TTF by the more polarizable selenium and tellurium, and the synthesis of vinylogs, heterocyclic bridged vinylogs, cyclophane-type molecules, and dendralene-type analogues such as **3** and **4**.[2]

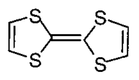

1

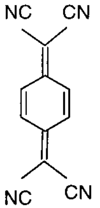

2

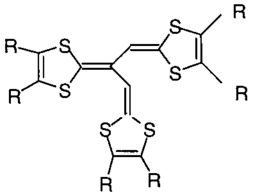

3a R = COOMe
3b R = H
3c R = -(CH=CH)$_2$

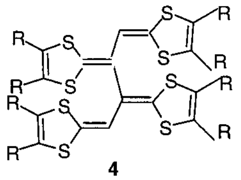

4

4a R = COOMe
4b R = H

The all-sulfur-containing [3]- and [4]dendralenes[3] were prepared by successive formylation and Wittig reactions on the known vinylog **8**[4] and the resulting [3]dendralenes. Since no selenium-containing analogues of **3** or **4** are known, our present investigation was concerned with achieving the synthesis of dendralene-type TTF vinylogs bearing a 1,3-diselenole moiety, exemplified by **5**−**7**, and studying the effects of structural perturbation on the electrochemistry of such systems.

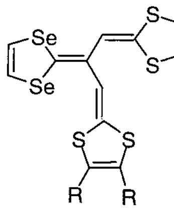

5 R = COOMe
6 R = H
7 R =-SCH$_2$CH$_2$S-

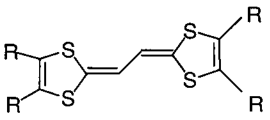

8 R = COOMe

Results and Discussion

An efficient synthesis of the selenium-containing [3]-dendralene **5** was achieved as follows. The known 2-methylene-1,3-diselenole **9**[5] was converted to the dialdehyde **10** in good yield under controlled conditions. However, initial attempts at condensing dialdehyde **10** with 4,5-dicarbomethoxy-1,3-dithiole-2-phosphorane under standard conditions using triethylamine gave only a monocondensed product **11**. Aldehyde **11** was also made from the known vinylog **12**.[6] A similar trend was observed in the case of the condensation of the dialdehyde with the phosphonium salt **13** and phosphonate **14**, when only monocondensed products **15** and **16** were obtained. To assess the reactivity of dialdehyde **10**, it was treated with the stable carbomethoxymethylphosphorane, and the expected biscondensation product **17** was obtained in 95% yield.

An added complication in these reactions was the known equilibrium between **13** and the corresponding thiolium salt, which condensed under the influence of the base to give BEDT.TTF.[7] The latter complication was avoided by use of the known phosphonate **18** in the presence of *n*-butyllithium. Again the use of stoichiometric amounts of the phosphonates **14** and **18** gave rise only to the monocondensation products **16** and **15**. The use of

---

(1) Ferraris, J. P.; Cowan, D. O.; Walatka, V.; Perlstein, J. H. *J. Am. Chem. Soc.* **1973**, *95*, 948.

(2) Schukat, G.; Fanghänel E. *Sulfur Rep.* **1996**, *18*, 1.

(3) Misaki, Y.; Matsumura, Y.; Sugimoto, T.; Yoshida, Z. *Tetrahedron Lett.* **1989**, *30*, 5289.

(4) Yoshida, Z.; Awaji, H., Sugimoto, T.; Yoshida, Z. *Tetrahedron Lett.* **1984**, *25*, 4227.

(5) Jackson, Y. A.; White, C. L.; Lakshmikantham, M. V.; Cava, M. P. *Tetrahedron Lett.* **1987**, *28*, 5635.

(6) Lakshmikantham, M. V.; Jackson, Y. A.; Cava, M. P. *J. Org. Chem.* **1988**, *53*, 3529.

(7) Hansen, T. K.; Lakshmikantham, M. V.; Cava, M. P.; Becher, J. *J. Am. Chem. Soc.* **1992**, *114*, 5035.

10.1021/jo010663e CCC: $20.00

Scheme 1

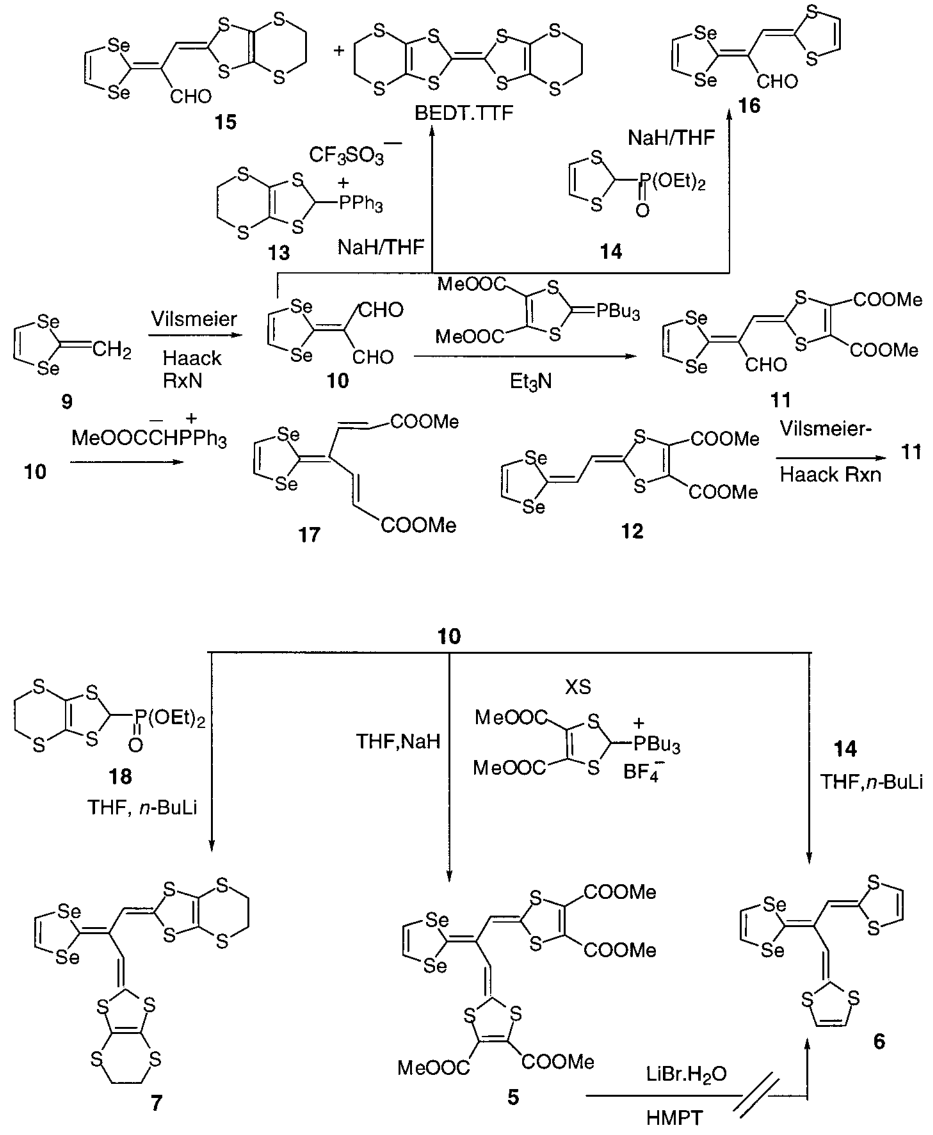

excess dicarbomethoxy-1,3-dithiole-2-phosphorane in the presence of sodium hydride gave the biscondensation product, namely [3]dendralene **5** in 88% yield. The [3]-dendralene **6** could not be synthesized by direct decarbomethoxylation of **5**. However, use of a 2-fold excess of the phosphonate **14** in the presence of *n*-butyllithium as the base gave **6** in 67% yield. Similarly, the reaction of **10** with an excess of phosphonate **18** in the presence of *n*-butyllithium produced the highly insoluble dendralene **7** in 58% yield (Scheme 1).

The monocondensation product **11** was converted to the totally unsymmetrical [3]dendralene **19** in 28% yield by reaction with phosphonate **18** in the presence of *n*-butyllithium. Thus, the aldehyde functionality in the monocondensation products can be elaborated into other unsymmetrical [3]dendralenes (Scheme 2).

An earlier report described the conversion of [3]-dendralenes to [4]dendralenes via the Vilsmeier−Haack, Wittig reaction route.[3] The extension of this approach to [3]dendralene **5** gave the aldehyde **20** in 59% yield; reaction of **20** with the diester dithiole phosphorane gave [4]dendralene **21** (Scheme 3).

Reductive cyclodimerization and cyclotrimerization of the dibromo derivative **22** catalyzed by a Ni catalyst to

Scheme 2

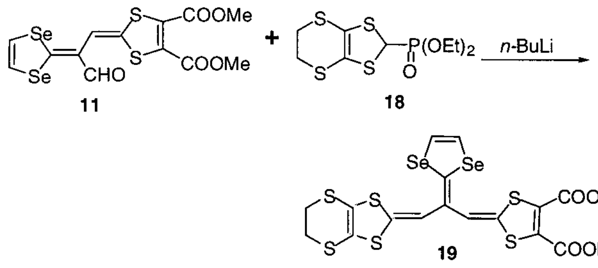

give radialene **23** and **24** have been described.[8] While dendralene **5** can be readily transformed to a dibromo derivative **25**, its reaction with Ni(0) does not lead to the expected dimeric product **26**, nor any other tangible product. However, it should be pointed out that the bromines in **25** are 1,3-related and not 1,2 (Scheme 4).

Electrochemical Studies. A typical cyclic voltammetric response of **5** on a Pt electrode in 0.1 M TBAHFP−

---

(8) (a) Sugimoto, T.; Awaji, H.; Misaki, Y.; Yoshida, Z.; Kai, Y.; Nakagawa, H.; Kasai, N. *J. Am. Chem. Soc.* **1985**, *107*, 5792. (b) Sugimoto, T.; Misaki, Y.; Kajita, T.; Yoshida, Z.; Kai, Y.; Kasai, N. *J. Am. Chem. Soc.* **1987**, *109*, 4106.

Scheme 3

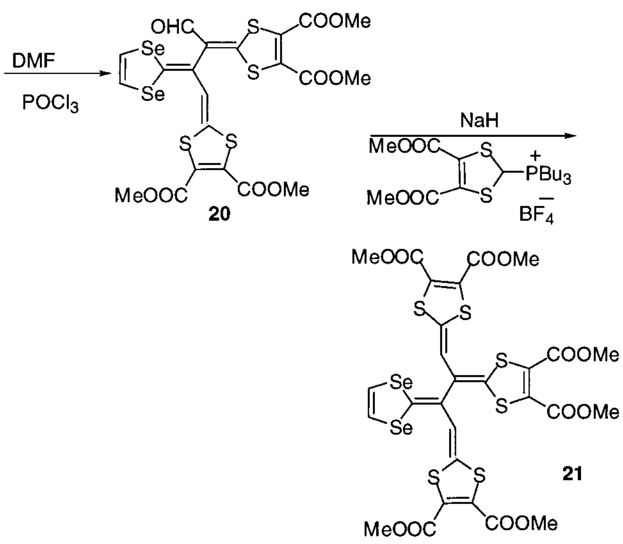

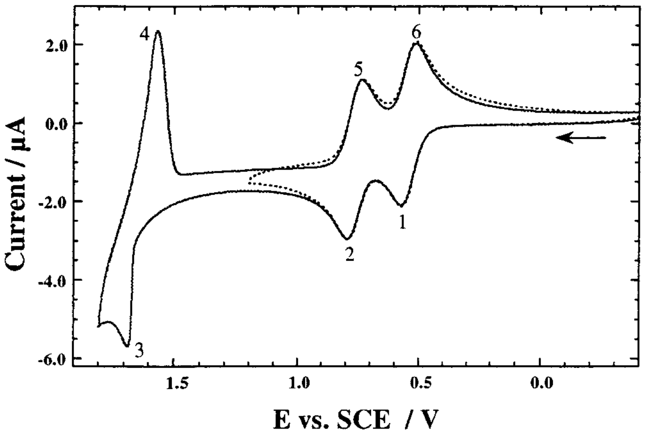

Figure 1. Cyclic voltammograms for 0.5 mM [3]dendralene **5** in 0.1 M TBAHFP−CH$_2$Cl$_2$. Scan rate: 0.05 V s^{-1}; potential window: −0.4 to +1.2 V for the dotted line. Solutions were prepared and measurements were conducted in a N$_2$-box. A Pt disk (diam 1.6 mm) was the working electrode, and SCE was the reference electrode.

CH$_2$Cl$_2$ solution is shown in Figure 1. During the anodic scan, there are three peaks 1, 2, and 3, with potentials of $E^a_{p1} = 0.573$ V; $E^a_{p2} = 0.796$ V; and $E^a_{p3} = 1.684$ V vs SCE, which correspond to three oxidation steps of the neutral species and the resulting radical cations and dications of **5.** During the cathodic scan, there are also three peaks, 4, 5, and 6, with potentials of $E^c_{p4} = 1.572$ V; $E^c_{p5} = 0.732$ V; and $E^c_{p6} = 0.512$ V vs SCE, which correspond to the reduction of the oxidized species. The slightly enhanced peak 4 may be due to adsorption or electrodeposition of species formed after the oxidation of the dication of **5**. The peak intensity ratio of I^c_{p6}/I^a_{p1}or I^c_{p5}/I^a_{p2} is close to 1, and changing the scan rate has little effect on these peak intensity ratios. Alteration of the potential window does not change the peak intensity

Scheme 4

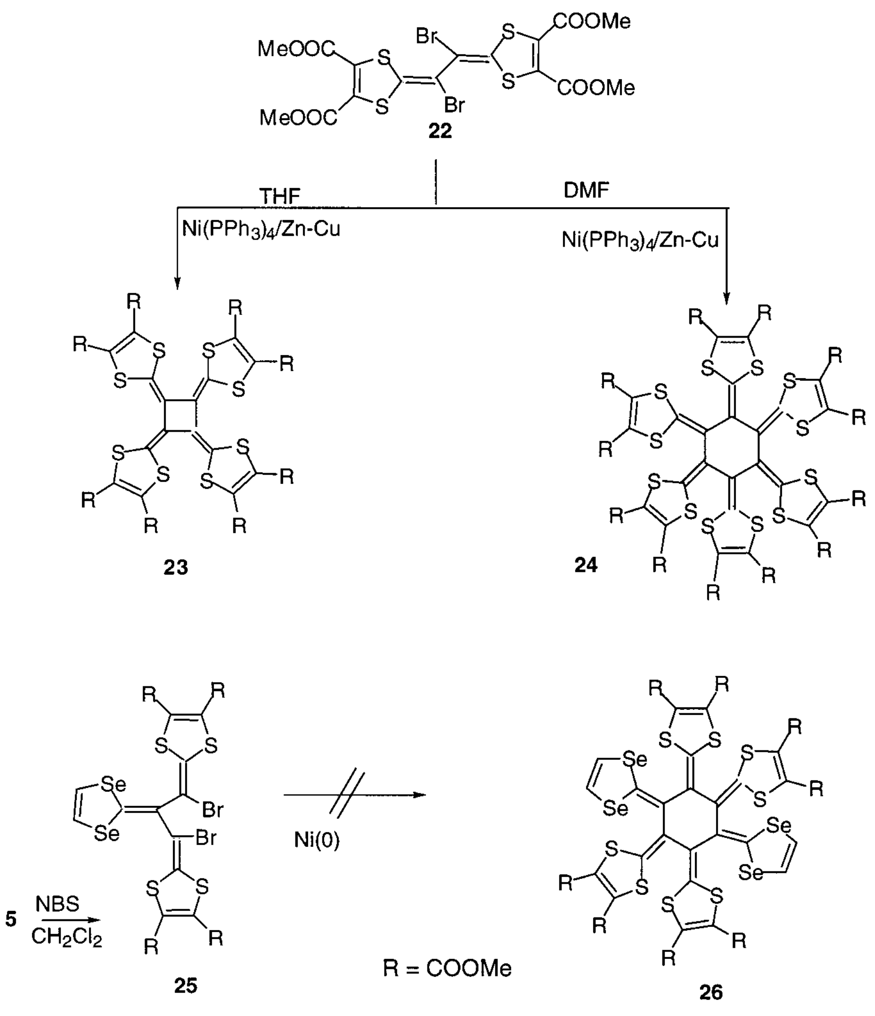

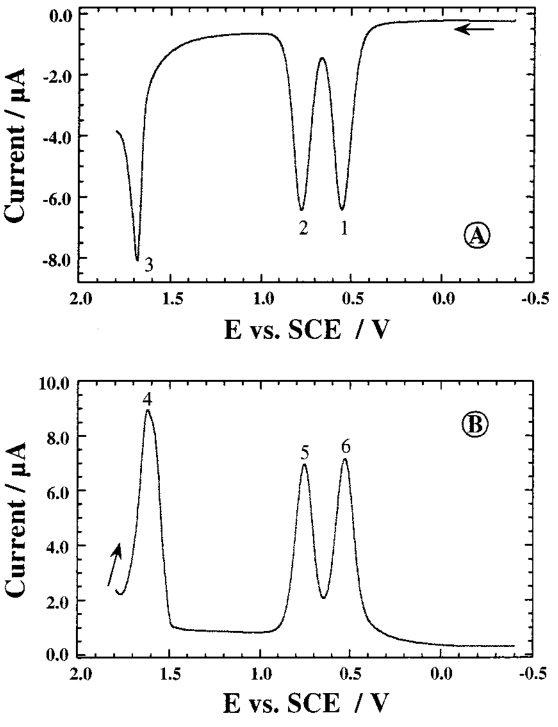

Figure 2. Osteryoung square wave voltammograms for 0.5 mM **5** in 0.1 M TBAHFP−$\mathrm{CH_2Cl_2}$. Potential scan in (A); −0.4 to +1.8 V, and (B): +1.8 to −0.4 V. Other experimental conditions are the same as in Figure 1.

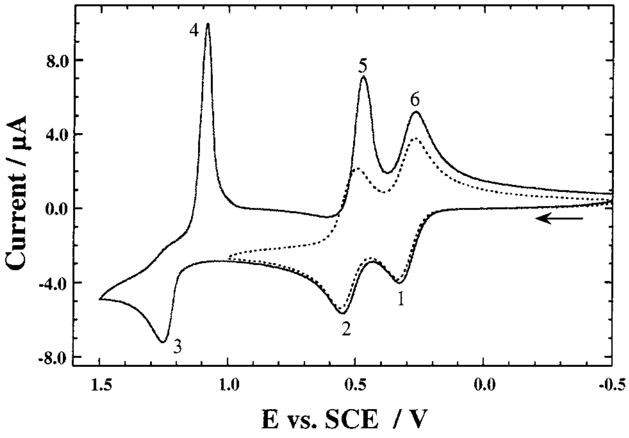

Figure 3. Cyclic voltammograms for 0.37 mM dendralene **6** in 0.1 M TBAHFP−$\mathrm{CH_2Cl_2}$. Scan rate: 0.05 V s^{-1}; potential window: −0.5 to +1.0 V for dotted line. Other experimental conditions are the same as in Figure 1.

(such as peaks 1, 2, 5, and 6, see dotted line in Figure 1). This implies that the radical cations and dications of **5** produced during the oxidation process are chemically stable, and their oxidation−reduction reactions can be considered to be quasireversible. The above three pairs of peaks can be clearly seen in Osteryoung square wave voltammograms (OSWV) depicted in Figure 2.

The CV of compound **6** (Figure 3) is similar to that of **5** and displays three pairs of peaks. On the other hand, all three cathodic peaks (4, 5, and 6) are enhanced when the switch potential is +1.5V vs SCE (solid line in Figure 3). When the potential window is −0.5−1.0 vs SCE, the CV shape (dotted line in Figure 3) is similar to those of compound **5**, i.e., the radical cations and dications of **6** produced during the oxidation process are chemically stable, and their oxidation−reduction reactions can be considered to be quasireversible. When scanning the potential to the more positive value of +1.5 V, the dications of **6** are oxidized to other species (such as trications, radical trications) which can produce dimers or polymers of **6**. The adsorption or electrodeposition of the above species on the electrode surface results in the enhanced peaks 5 and 6. By comparing the structures of **6** and **5,** which are shown in Scheme 1, it is understandable that compound **6** can more easily form dimers or polymers after electrochemical oxidation than compound **5** because of a space effect produced by four substituted ester groups in **5**. The Osteryoung square wave voltammograms of compound **6** (Figure 4) are similar to those of compound **5** (Figure 2) except there is a shoulder peak accompanying peaks 3 and 4.

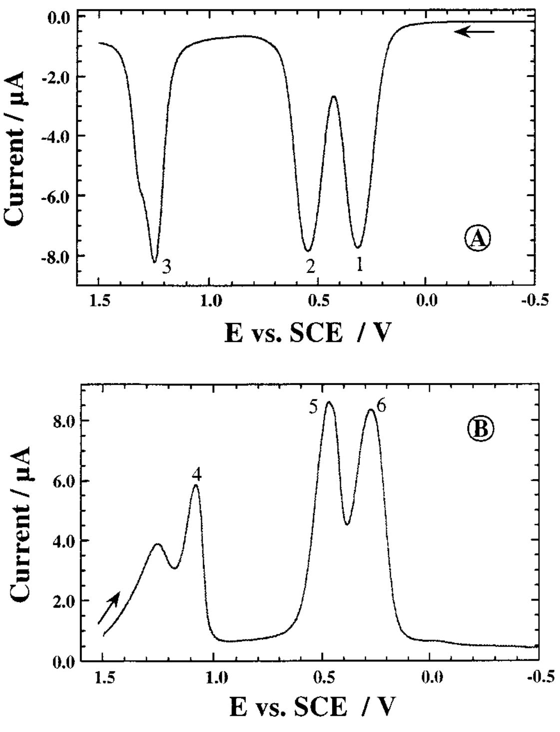

Figure 4. Osteryoung square wave voltammograms for 0.37 mM [3]dendralene **6** in 0.1 M TBAHFP−$\mathrm{CH_2Cl_2}$. Potential scan in (A): −0.5 to +1.5 V, and (B): +1.5 to −0.5 V. Other experimental conditions are the same as in Figure 1.

Compound **7** is insoluble in all solvents. Conventional electrochemical techniques are not suitable for this special compound. In the present work, electrochemical studies of **7** were carried out by mechanically attaching the solid powder to the Pt electrode surface. Its typical cyclic voltammogram is depicted in Figure 5 (solid line). In the potential window, one anodic peak (1), and two cathodic peaks (2 and 3) were observed. The oxidation potential is 0.43 ± 0.02 V vs. SCE. Actually, the redox reaction of **7** consists of multielectron-transfer processes as evidenced by its Osteryoung square wave voltammograms (Figure 6) that show several shoulders on peaks 1 and 2.

The oxidation potentials of [3]dendralenes **5**, **6**, and **7** as well as **3a**, **3b**, and **3c** are presented in Table 1. The first (E°_1) and second (E°_2) oxidation potentials for **6** are 240 mV more negative, and the third (E°_3) oxidation potential is 470 mV more negative than those for **5.** Therefore, the absence of the four ester groups makes **6** more susceptible to oxidation than **5.**

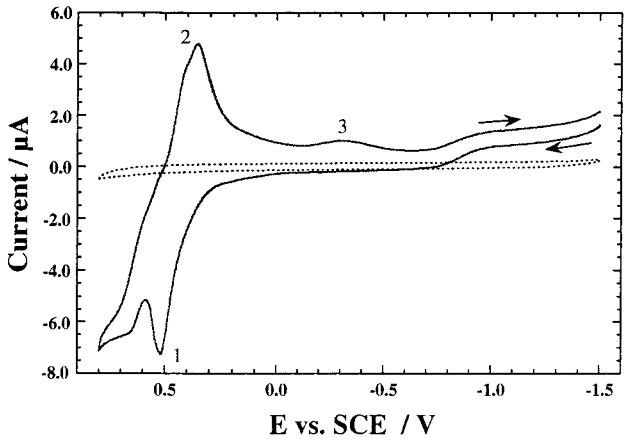

Figure 5. Cyclic votammograms for Pt disk (dia. 1.6 mm) electrode modified with dendralene **7** film (solid line) and bare Pt disk electrode (dotted line) in 0.2 M $TBAClO_4$−propylene carbonate solution. Scan rate: 0.05 V s^{-1}. The solution was purged with argon for 15 min before measurement.

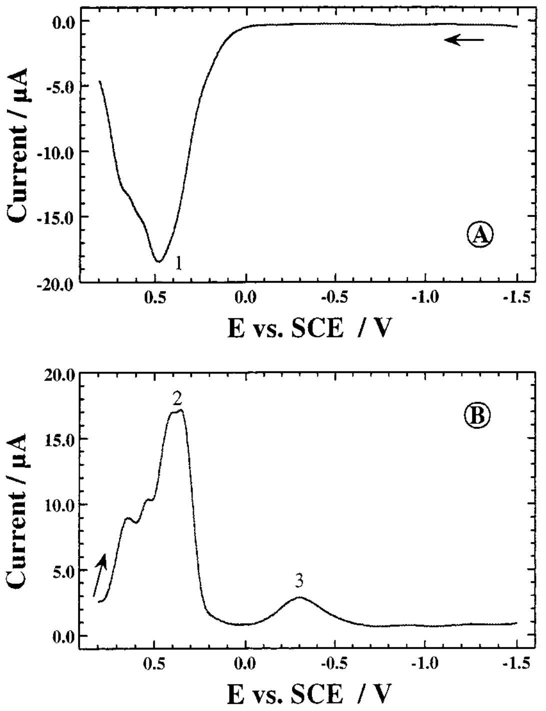

Figure 6. Osteryoung square wave voltammograms for Pt disk (1.6 mm) modified with a film of **7** in 0.2 M $TBAClO_4$−propylene carbonate solution. Potential scan in (A): −1.5 to +0.8 V, and (B): +0.8 to −1.5 V. Other experimental conditions are the same as in Figure 5.

Comparison of the oxidation potentials of **5** (entry 1) to **3a** (entry 4) shows that the replacement of one diester-carrying 1,3-dithiole unit lowers E°_1 by ∼150 mV, E°_2 by 10 mV and E^O_3 by 100 mV. In contrast, E°_1 in **6** (entry 2) is 48 mV higher than in **3b** (entry 5) due to the replacement of a 1,3-dithiole unit by a 1,3-diselenole unit reflecting the difference in the polarizability of selenium versus sulfur. This effect is also seen in the second oxidation potential in **3b** (0.40 V) versus E°_2 in **6** (0.523 V), Δ being ∼ 120 mV as well as E°_3 in **6** being 145 mV higher than in **3b**. A comparison of **7** cannot be made since the corresponding all sulfur analogue is unknown.

Table 1. Oxidation Potentials of [3]Dendralenes[a]

entry	compd	E°_1/V	E°_2/V	E°_3/V	ref
1	**5**	0.551 ± 0.010	0.780 ± 0.013	1.646 ± 0.019	
	5[b]	0.538 ± 0.005	0.765 ± 0.008	1.645 ± 0.023	
2	**6**	0.308 ± 0.010	0.523 ± 0.019	1.175 ± 0.023	
3	**7**	0.43 ± 0.02			
4	**3a**	0.70	0.79	1.75	3, 11
5	**3b**	0.26	0.40	1.32	3, 11
6	**3c**	0.50	0.62	1.53	3, 11

[a] A Pt disk (dia. 1.6 mm) was used as the working electrode except as noted. SCE was the reference electrode in all experiments. The above potentials were estimated from CVs and OSWVs. [b] Glassy carbon disk (dia. 3.0 mm) was used as the working electrode.

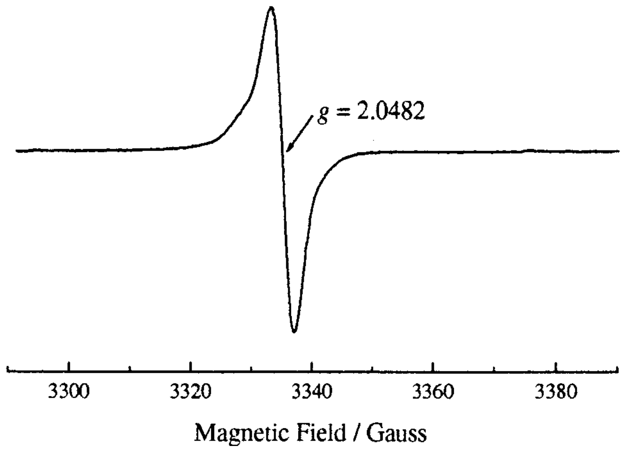

Figure 7. EPR spectrum of $6^{\bullet+}$ generated by bulk electrolysis at 430 mV (microwave frequency 9.5 GHz, microwave power 5 mW, modulation 2G).

EPR Measurements. Radical cations of the dendralenes **5** and **6** were detected during SEEPR measurements. The originally yellow solutions changed to violet immediately after starting bulk electrolysis. The EPR spectrum of the tetraester dendralene radical cation generated in 2 × 10^{-3} M CH_2Cl_2 solution at 580 mV exhibited a single line with *g* value 2.0482 (Figure 7). This is an average between the *g* values of sulfur-containing (2.02)[9] and selenium-containing radicals (2.08).[10] The radical cation of the dendralene **6** generated in 1.5 × 10^{-3} M CH_2Cl_2 solution at 340 mV gives an EPR signal with *g* value 2.0172 which is characteristic of sulfur-containing radicals (Figure 8).

We carried out PM3 geometry optimization of the compounds **5** and **6** and their radical cations by using *HyperChem* Molecular Modeling System (Release 6.03). Figures 9 and 10 show the geometry optimized structures of $\mathbf{5}^{\bullet+}$ and $\mathbf{6}^{\bullet+}$, respectively. Parameters of $\mathbf{5}/\mathbf{5}^{\bullet+}$ and $\mathbf{6}/\mathbf{6}^{\bullet+}$ compounds are present in Table 2.

The spin density distribution in $\mathbf{5}^{\bullet+}$ and $6^{\bullet+}$ radical cations estimated by UHF/PM3 calculations demonstrated that in both compounds the spin density is delocalized over the entire molecule. This is in a good agreement with EPR measurements for $\mathbf{5}^{\bullet+}$. However, for $6^{\bullet+}$ the experimental *g* value shows that the spin population is higher on sulfur atoms. The difference between heats of formation $\Delta H_{5/5}{}^{\bullet+}$ ($\Delta H_5{}^{\bullet+}$ − ΔH_5 = 184.5 kcal/

---

(9) (a) Windle, J. J.; Wiersema, A. K.; Tappel, A. L. *J. Chem. Phys.* **1964**, *41*, 1996. (b) Henriksen, T. *J. Chem. Phys.* **1962**, *37*, 2189.

(10) Stiles, D. A.; Tyerman, W. J. R.; Strausz, O. P.; Gunning, H. E. *Can. J. Chem.* **1966**, *44*, 2149.

(11) The reported oxidation potentials in ref 3 were obtained by cyclic voltammetry in benzonitrile solution using Pt working and counter electrodes and tetrabutylammonium perchlorate as an electrolyte and SCE as reference electrode.

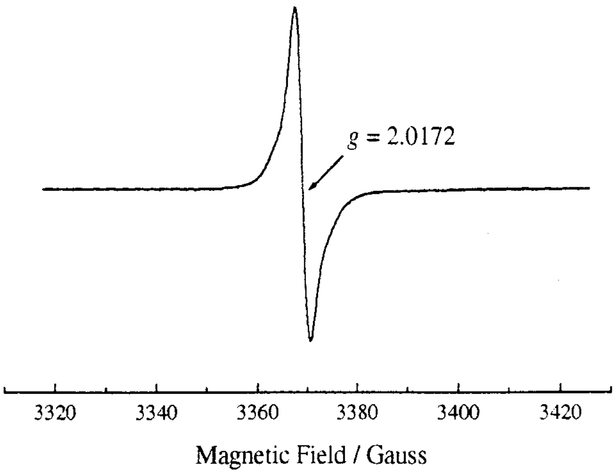

Figure 8. EPR spectrum of $5^{\bullet+}$ generated by bulk electrolysis at 580 mV (microwave frequency 9.5G Hz, microwave power 5 mW, modulation 2G).

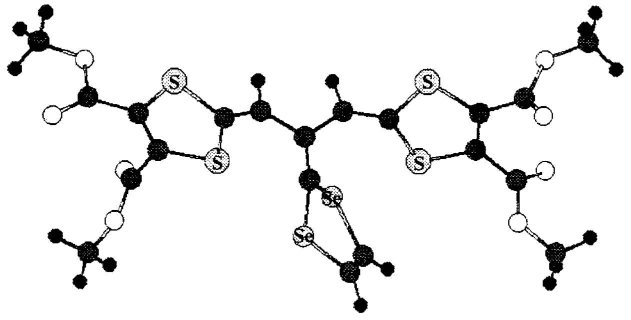

Figure 9. PM3-optimized geometry of $5^{\bullet+}$. Big black circles are carbon atoms, small black circles are hydrogen atoms, white circles are oxygen atoms.

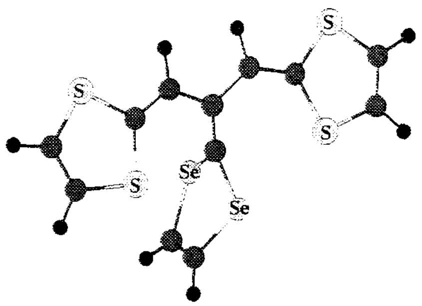

Figure 10. PM3-optimized geometry of $6^{\bullet+}$. Big black circles are carbon atoms, small black circles are hydrogen atoms.

Table 2. Parameters of PM3-Optimized Structures for Compunds 5 and 6

	5	5^{+}	6	6^{+}
heat of formation (kcal/mol)	−224.25	−39.77	77.91	261.11
HOMO (eV)	−8.426		−8.011	
dipole moment (Debye)	1.188	2.105	1.154	3.096

mol) is larger that $\Delta H_{6/6}{}^{\bullet+} = 183.2$ kcal/mol. Ionization potential of **5** ($I_p = 8.426$ eV) obtained from semiempirical calculations is also greater than that of **6** ($I_p = 8.011$ eV). This correlates well with their first oxidation potentials measured electrochemically.

The presence of four electron-withdrawing ester groups (COOMe) leads to increase of the oxidation potential of **5** as well as ionization potential compared to **6**.

Table 3. Optical Properties of 5, 6, and 7

compd	ϵ	λ	solvent
5	$(1.86 \pm 0.02) \times 10^4$	404	dichloromethane
6	$(3.57 \pm 0.03) \times 10^4$	407	dichloromethane
7[a]	-	409	dichloromethane

[a] A saturated solution was used for optical measurements since only very little of compound **7** can be dissolved in any organic solvent. All measurements were conducted at room temperature (24 ± 2 °C).

Optical Measurements. The optical spectrum of **5** shows absorption at $\lambda_{\max} = 404$ nm, 240 nm, and one of lower intensity at 293 nm. For neutral **6**, the absorption maxima occur at 407, 303, and 241 nm. The peak intensity at 241 nm is weaker in comparison to that of **5**. Compound **7** is insoluble in most solvents. However, it is slightly soluble in propylene carbonate (PC). Hence, a saturated solution was prepared by placing **7** in PC and then sonicating the mixture for over 30 min. The top clear solution was used for optical measurements. The spectrum of **7** shows maxima at 409, 310, and 215 nm. In contrast to compounds **5** and **6**, the 409 nm peak is broad, 215 nm is a maximum peak and also blue shifted, and 310 nm becomes a shoulder peak. The molar extinction coefficients and characteristic absorption maxima are summarized in Table 3.

Conclusions

Several selenium containing [3]dendralene TTF vinylogs have been prepared via Wittig and Wittig/Horner reactions, and their electrochemical behavior was studied. Comparison of the oxidation potentials of the [3]-dendralenes **5** and **6** with the known sulfur analogues **3a** and **3b** showed that the perturbation caused by the replacement of sulfur by selenium lowers the oxidation potentials. The *g* value for the radical cation of **5** is 2.048 and is larger than that of the radical cation of **6** (2.017) and is an average between organic S radicals and Se radicals. MO calculations indicate larger spin density on the selenium atom compared to sulfur. The difference between the calculated ionization potentials of **5** and **6** is in agreement with the difference in their oxidation potentials.

Experimental Section

General Comments. Melting points are uncorrected. THF was freshly distilled from sodium−benzophenone. All mass peaks containing Se are reported for ^{80}Se.

2-(1,1-Diformylmethylene)-1,3-diselenole (10). Phosphorus oxychloride (4.59 mL, 49.2 mmol) was added slowly over a period of 20 min to DMF (10.2 mL, 31.2 mmol) cooled in an ice bath. To this mixture was slowly added a solution of 2-methylenediselenole **9**[5] (9.45 g, 16.4 mmol) in DMF (13 mL). The mixture was warmed to room temperature and was maintained at 60 °C overnight. The reaction mixture was poured into ice−water and neutralized to pH 7 by using 10% sodium hydroxide solution. The crude solid was filtered, washed with water, and chromatographed (80:20 chloroform hexane) to give a 70% yield of dialdehyde **10** as a yellow solid along with traces of monoaldehyde. An analytical sample of **10** was obtained by recrystallization (chloroform−hexane) mp 248−249 °C (decomp); ^{1}H NMR ($CDCl_3$) δ 9.91 (s, 2H), 8.46 (s, 2H); ^{13}C NMR ($CDCl_3$) δ 184.92, 180.81, 133.0, 132.34, 127.77; IR (KBr) ν 1649, 1591, 1384 cm^{-1}; UV−vis (CH_2Cl_2) $\lambda_{\max}$ nm (log ϵ) 400 (3.66), 268 (3.85), 252 (3.84); MS *m/z* (relative intensity) 268 (M^+, 50), 240 (100), 212 (19), 184 (23), 160 (45), 130 (29). Anal. Calcd for $C_6H_4O_2Se_2$; C, 27.10; H, 1.51. Found: C, 27.17; H,1.61.

Propylidene-1,3-bis(4,5-dicarbomethoxy-1,3-dithiole)-2-(1,3-diselenole) 5. To a stirred suspension of hexane-washed NaH (0.492 g, 12.2 mmol) in THF (8 mL) was added slowly the diester phosphonium salt (4.538 g, 9.02 mmol) in THF (78 mL) at room temperature. After stirring 10 min, a solution of dialdehyde **10** (1.0 g, 3.7 mmol) in THF (105 mL) was added to the reaction mixture over a period of 15−20 min. The mixture was stirred for 3−4 h. After quenching the reaction mixture with satd ammonium chloride solution, the solvent was removed. Standard workup yielded the crude product, which was triturated with methanol to furnish dendralene **5** (88% yield). An analytical sample of **5** was obtained by crystallization from methanol−dichloromethane as a reddish brown solid; mp 105.7−106.2 °C; ^{1}H NMR ($CDCl_3$) δ 7.26 (s, 2H), 5.66 (s, 2H), 3.839 (s, 6H), 3.834, (s, 6H); ^{13}C NMR ($CDCl_3$) δ 159.99, 134.16, 134.15, 134.13, 132.28, 131.71, 130.33, 122.56, 110.76, 53.27, 53.22; MS *m/z* (relative intensity) 672 (M^+, 42), 670 (100), 485 (66), 448 (38); IR (KBr) ν 1745, 1719, 1579 cm^{-1}; UV−vis (CH_2Cl_2) $\lambda_{\max}$ nm (log ϵ) 398(4.63), 287(4.65). HRMS Calcd for $C_{20}H_{16}O_8S_4Se_2$ 671.8058, found 671.8079.

Dendralene 6. A hexane solution of *n*-BuLi (0.7 mL, 2.5 M) was added to a solution of phosphonate **14** (0.34 g, 1.77 mmol) in THF (10 mL) at −78 °C. A solution of dialdehyde **10** (0.094 g, 0.354 mmol) in THF (12 mL) was added during 10 min to the phosphorane generated above at −78 °C. The mixture was warmed gradually to room temperature. The solvent was evaporated. After standard workup, the crude product was subjected to chromatography (1:1 dichloromethane: hexane) under a nitrogen atmosphere to afford dendralene **6** as a yellow solid, mp 156.7−158.3 °C; ^{1}H NMR (C_6D_6) δ 6.47 (s, 2H), 6.01 (s, 2H), 5.42 (s, 4H); ^{13}C NMR (C_6D_6) δ 141.21, 123.02, 122.42, 119.64, 117.04, 110.05; MS *m/z* (relative intensity) 440 (M^+, 100), 149 (14); IR (KBr) ν 1547, 1485 cm^{-1}; UV−vis (CH_2Cl_2) $\lambda_{\max}$ nm (log ϵ) 402 (4.28), 299 (4.35); HRMS Calcd for $C_{12}H_8S_4Se_2$: 437.7847. Found 437.7829.

Dendralene 7. To a stirred suspension of hexane-washed NaH (0.0409 g, 0.9 mmol) in THF (1 mL) was added slowly phosphonate **18** (0.297 g, 0.9 mmol) in THF (5 mL) at room temperature. After stirring 10 min, a solution of dialdehyde **10** (0.059 g, 0.22 mmol) in THF (10 mL) was added slowly. The reaction mixture was stirred further for 1 h. A yellow solid separated from the reaction mixture and was filtered and dried. The crude solid was washed with hot chlorobenzene to remove the impurities to give dendralene **7** in 58% yield. mp 233.1−233.3 °C; MS *m/z* (relative intensity) 620 (M^+, 12), 619 (22), 591 (15), 395 (15), 319 (31), 295 (50), 223 (30), 206 (100), 178 (95), 148 (75); IR (KBr) ν 1483, 1402 cm^{-1}. Anal. Calcd for $C_{16}H_{12}S_8Se_2$: C, 31.06; H, 1.95. Found: C, 31.71; H, 2.08.

Aldehyde 16. To a suspension of NaH (0.081 g, 1.77 mmol) in THF (3 mL) was added phosphonate **14** (0.34 g, 1.77 mmol) in THF (4 mL). The solution was stirred for 15 min, and a solution of dialdehyde **10** (0.117 g, 0.4 mmol) in THF (12 mL) was added slowly over a period of 15 min. After 1/2 h, the solution was diluted with aq NH_4Cl and extracted with CH_2Cl_2 (3 × 25 mL). The combined organic extracts were dried (Na_2SO_4) and evaporated. The crude solid was purified by column chromatography (6:4 dichloromethane:hexane) under a N_2 atmosphere to give aldehyde **16** (67%) as an orange-red solid, mp 103.9−104.4 °C; ^{1}H NMR ($CDCl_3$) δ 9.51 (s, 1H), 7.90 (d, 1H, J = 7.2 Hz), 7.73 (d, 1H, J = 7.2 Hz), 6.26 (d, 1H, J = 2 Hz), 6.20 (d, 1H, J = 2 Hz), 6.07 (s, 1H); ^{13}C NMR ($CDCl_3$) δ 182.57, 130.04, 125.92, 122.20, 117.80, 117.69, 109.43; MS *m/z* (relative intensity) 354 (M^+, 88), 352 (100), 325 (24), 221 (52), 140 (39), 116 (21); IR (KBr) ν 1615, 1562, 1418 cm^{-1}; UV−vis (CH_2Cl_2) $\lambda_{\max}$ nm (log ϵ) 443 (4.42), 361 (4.38), 264 (4.11); HRMS: Calcd for $C_9H_6OS_2Se_2$: 353.819. Found 353.8201.

Aldehyde 11. Method A. To a mixture of dialdehyde **10** (0.10 g, 0.375 mmol) and triethylamine (0.483 mL) in THF (3 mL) was added the diester phosphonium salt (0.685 g, 1.35 mmol). The solvent was evaporated, and the crude product was chromatographed (7:3 hexane:ethyl acetate) to give **11** (18%); mp 162.9−163.1 °C; ^{1}H NMR ($CDCl_3$) δ 9.48 (s,1H), 7.95 (d, 1H J = 7.2Hz), 7.78 (d, 1H, J = 7.2 Hz), 6.05 (s, 1H), 3.85 (s, 3H), 3.79 (s, 3H); ^{13}C NMR ($CDCl_3$) δ 181.25, 162.07, 159.80, 159.58, 135.39, 131.03, 130.39, 129.98, 124.28, 122.62, 112.13, 53.33, 53.22; MS *m/z* (relative intensity) 470 (M^+, 100), 464 (24), 441 (16), 335 (20), 256 (21), 232 (14), 221 (56), 149 (43), 117 (25); IR (KBr) ν 1726, 1707, 1609, 1582 cm^{-1}; UV−vis (CH_2Cl_2) $\lambda_{\max}$ nm (log ϵ) 399(4.49), 272 (4.11). HRMS Calcd for $C_{13}H_{10}O_5S_2Se_2$ 469.830. Found 469.8316.

Method B. Phosphorus oxychloride (0.103 mL, 1.1 mmol) was added slowly to a stirred solution of DMF (0.395 mL, 5.09 mmol) in CH_2Cl_2 (2 mL) kept at 0−5 °C. After the addition was over, the mixture was warmed to 35 °C to complete the formation of the Vilsmeier reagent. A solution of the vinylog **12**[4] (0.045 g, 0.101 mmol) in CH_2Cl_2 (3 mL) was added slowly to the ice-cooled solution of the above reagent. The mixture was slowly warmed to room temperature and maintained for 4 h. The solvent was evaporated, the residue was poured into ice−water, and the pH was adjusted to 7 with 10% aqueous NaOH solution. The crude product was filtered and washed with water. Purification was achieved by column chromatography, 7:3 hexane:ethyl acetate) to give aldehyde **11** in 70% yield, identical with the monocondensation product described above.

Aldehyde 15. To a mixture of dialdehyde **10** (0.075 g, 0.28 mmol) and phosphonium salt **13** (0.42 g 0.70 mmol) in THF (25 mL) was added triethylamine (0.196 mL). After 1.25 h stirring, the red solid (BEDT.TTF) was filtered. The crude product isolated from the filtrate was purified by column chromatography (7:3 hexane:dichloromethane) to give **15** in 13% yield; mp 166−167.5 °C; ^{1}H NMR ($CDCl_3$) δ 9.49 (s, 1H), 7.92 (d, 1H, J = 7.2 Hz), 7.75 (d, 1H, J = 7.2 Hz), 6.09 (s, 1H), 3.30 (s, 4H); MS *m/z* (relative intensity) 444 (M^+, 18), 443 (39), 415 (23), 352 (15), 248 (22), 223 (100), 206 (35), 188 (30), 136 (21); IR (KBr) ν 1592, 1219 cm^{-1}, HRMS Calcd for $C_{11}H_8OS_4Se_2$ 443.778. Found 443.779.

Diester 17. To a stirred solution of carbomethoxymethyl phosphorane (0.219 g, 0.657 mmol) in DMF (3 mL) was added a solution of dialdehyde **10** (0.07 g, 0.263 mmol) in DMF (3 mL). After stirring 3 h at room temperature, the mixture was heated to 65−70 °C for 5 h. The reaction mixture was poured into crushed ice and water. The yellow solid was filtered and washed. The crude product was purified by column chromatography (9:1 hexane:dichloromethane) to afford **17** as a yellow solid in 95% yield, mp 162.2.°C; ^{1}H NMR ($CDCl_3$) δ 7.48 (s, 2H), 7.34 (s, 1H), 7.3 (s, 1H), 6.30 (s, 1H), 5.99(s, 1H), 3.78 (s, 6H); ^{13}C NMR ($CDCl_3$) δ 183.32, 167.48, 152.21, 141.22, 140.73, 131.68, 124.44, 123.3, 118.11, 113.80, 51.69; MS *m/z* (relative intensity) 380 (M^+, 66), 347 (21), 321(100), 289 (59), 262 (48), 179 (61), 156 (491), 131 (30); IR (KBr) ν 1711, 1605, 1460 cm^{-1}; UV−vis (CH_2Cl_2) $\lambda_{\max}$ nm (log ϵ) 414 (3.19), 258 (3.16). Anal. Calcd for $C_{12}H_{12}O_4Se_2$: C, 38.10; H, 3.20. Found: C, 38.01; H, 3.25.

[3]Dendralene 19. *n*-Butyllithium solution (0.33 mL, 2.5 M) was added slowly to a solution of phosphonate **18** (0.24 g, 0.74 mmol) in THF (8 mL) at −78 °C. After 5 min stirring, a solution of aldehyde **11** (0.087 g, 0.18 mmol) in THF (9 mL) was added slowly. The reaction mixture was gradually warmed to room temperature and stirred for 1 h. After standard workup, the crude product was subjected to column chromatography to give **19** in 28% yield; mp 168.2 °C; ^{1}H NMR (DMSO-d_6) δ 7.26 (s, 2H), 5.68 (s, 2H), 3.82 (s, 6H), 3.29 (s, 4H); ^{13}C NMR (DMSO-d_6) δ 160.22, 160.05, 132.11, 129.99, 122.47, 122.41, 111.01, 53.24, 29.76, 29.63 ppm; MS *m/z* (relative intensity), 646 (M^+, 26), 645 (49), 614 (20), 448 (22), 392 (39), 368 (47), 311 (32), 278 (42), 206 (72), 174 (27), 155 (70), 125 (100). IR (KBr) ν 1730, 1715, 1540 cm^{-1}; UV−vis $\lambda_{\max}$ nm (log ϵ) 412 (4.79), 302 (4.71). HRMS Calcd for $C_{18}H_{14}O_4S_6Se_2$ 645 7546. Found 645.7547.

[3]Dendralene Aldehyde 20. To a stirred solution of dimethyl formamide (0.36 mL, 5.0 mmol) in dichloromethane (1 mL) was added slowly phosphorus oxychloride (0.046 mL, 0.5 mmol) under ice cold conditions. After the addition, the mixture was slowly heated to 35 °C for completion of the Vilsmeier reagent formation. The reaction mixture was recooled to 0−5 °C, and a solution of [3] dendralene **5** (0.168 g, 0.25 mmol) in dichloromethane (3 mL) was added. After 2 h at room temperature, standard workup followed by column chromatography (SiO_2, hexane:ethyl acetate 7:3) gave aldehyde **20** as a reddish-brown solid in 59% yield; mp 93−93.5 °C; ^1H NMR ($CDCl_3$) δ 9.23 (s, 1H), 7.27 (d, 1H, $J = 7.2$ Hz), 7.20 (d, 1H, $J = 7.2$ Hz), 5.89 (s, 1H), 3.93 (s, 3H), 3.90 (s, 3H), 3.80 (s, 3H), 3.77 (s, 3H); ^{13}C NMR ($CDCl_3$) δ 184.06, 159.90, 159.43, 137.41, 136.43, 131.69, 130.80, 129.73, 128.88, 122.49, 122.43, 118.72, 110.89, 53.62, 53.30, 53.26; MS *m*/*z* (relative intensity) 700 (M^+, 11), 532 (6), 494 (15), 436 (12), 392 (20), 250 (21), 149 (61), 110 (100); IR ν 1734, 1728, 1720, 1578, 1542 cm^{-1}; UV−vis λ_{max} nm (log ϵ) 384 (4.48). Anal. Calcd for $C_{21}H_{16}O_9S_4Se_2$. C, 36.10; H, 2.31; S, 18.36. Found: C; 36.42; H, 2.59; S, 18.06.

[4]**Dendralene 21.** A solution of the diester phosphonium salt (0.101 g, 0.2 mmol) in THF (3 mL) was added slowly at room temperature to a stirred suspension of hexane-washed NaH (0.0096 g, 0.2 mmol) in THF (3 mL). A solution of aldehyde **20** (0.07 g 0.1 mmol) in THF (3 mL) was added to the phosphorane. After 3−4 h at room temperature, aqueous NH_4Cl was added. Removal of the solvent and trituration of the resulting solid with methanol gave dendralene **21** in 77% yield, which was crystallized from methanol−dichloromethane; mp 103.2 °C; ^1H NMR ($CDCl_3$) δ 7.26 (s, 2H), 5.64 (s, 2H), 3.849, (s, 3H), 3.483 (s, 3H), 3.823 (s, 3H), 3.819 (s, 3H), 3.812 (s, 3H); ^{13}C NMR ($CDCl_3$) δ 160.86, 160.19, 160.09, 160.02, 159.92, 159.50, 137.61, 137.56, 134.90, 133.68, 132.83, 132.22, 130.71, 130.37, 129.62, 129.29, 127.66, 126.36, 124.77, 124.54, 123.57, 123.10, 121.93, 120.53, 110.77, 53.49, 53.45, 53.30; 53.22, 53.10; MS *m*/*z* (relative intensity) 902 (M^+, 1) 878 (52), 842 (27), 692 (39), 616 (48), 478 (19), 451 (40), 393 (25), 336 (29). 280 (52), 206 (39), 190 (100),117 (78); IR (KBr) ν 1725, 1577, 1432, 1255 cm^{-1}; UV−vis (CH_2Cl_2) λ_{max} nm (log ϵ) 390 (5.02), 297 (4.82). Anal. Calcd for $C_{28}H_{22}O_{12}S_6Se_2$: C, 37.31; H, 2.46; S, 21.36. Found: C, 37.20; H, 2.60; S, 21.29.

Dibromo[3]dendralene 25. A mixture of dendralene **5** (0.168 g. 0.25 mmol) and NBS (0.046 g, 0.525 mmol) in CH_2Cl_2 (4 mL) was refluxed under irradiation for 15 min. The organic layer was washed with water (2 × 10 mL) and dried over sodium sulfate. Evaporation of the solvent gave **25** (quantitative), mp 91.9−92.5 °C; ^1H NMR ($CDCl_3$) δ 7.48 (s, 2H), 3.85 (s, 6H), 3.83 (s, 6H); ^{13}C NMR ($CDCl_3$) δ 159.88, 159.53, 146.55, 135.62, 133.08, 129.46, 124.10, 122.46, 53.33, 53.07; MS *m*/*z* (relative intensity) 830 (M^+,3), 829 (11), 751 (8), 700 (6), 670 (44), 250 (13), 223 (17), 149 (24), 110 (100); IR (KBr) ν 1725, 1583, 1432, 1256 cm^{-1}; UV−vis (CH_2Cl_2) λ_{max} nm (log ϵ) 395 (5.96),350 (5.98), 287 (5.73). Anal. Calcd for $C_{20}H_{14}Br_2O_8S_4Se_2$: C, 29.00; H, 1.70; S, 15.48: Found: C, 29.79; H, 2.06: S, 15.4.

Electrochemical Studies. Chemicals. Tetrabutylammonium hexafluorophosphate (TBAHFP) was purchased from Fluka. Tetrabutylammonium perchlorate ($TBAClO_4$) was purchased from Alfa. Anhydrous dichloromethane (99.8%, CH_2Cl_2) and anhydrous propylene carbonate (PC) were obtained from Aldrich.

Electrochemical measurements were carried out in a three-electrode system at room temperature (24 ± 2 °C) by using a BAS-100 B/W electrochemical analyzer. For voltammetric measurements, a Pt disk (dia. 1.8 mm), or a glassy carbon (dia. 3.0 mm), or a film-coated Pt electrode were used as the working electrode. A saturated calomel electrode (SCE) and a platinum wire were used as reference and counter electrodes, respectively. Solutions containing **5** and **6** in 0.1 M TBAHFP−CH_2Cl_2 were prepared in a drybox under a nitrogen atmosphere. Solutions of $TBAClO_4$−PC were purged with high purity argon (99.998%, Post Airgas, Inc.) for 15 min to remove dissolved oxygen just before measurement.

Treatment of Working Electrode. The Pt disk electrode was polished with a soft polishing cloth by using METADI SUPREME polycrystalline diamond suspensions (water base) (BUEHLER) which include 3 and 1 μm diameter particles, starting with the 3 μm diameter particle suspension to polish for 5 min, and then 1 μm particles. After being polished, the disk electrode was washed thoroughly with deionized water and sonicated in deionized water for 3 min. The electrode was then rinsed with deionized water and anhydrous ethanol and was dried in a stream of argon just before use.

Preparation of Film-Coated Pt Electrode. The Pt electrode (diameter 1.8 mm) was pretreated as above. Then, a small amount of the solid powder of **7** was placed on a clean glass slide, and the Pt electrode surface was pressed on the fine powder, thereby causing some of compound **7** to adhere to the electrode surface to from a visible thin film.

EPR Measurements. EPR measurements were carried out with an X-band (9.5 GHz) Varian E-12 EPR spectrometer, equipped with a rectangular cavity. The magnetic field was measured with a Bruker EPR 035M gaussmeter, and the microwave frequency was measured with a model HP 5245L frequency counter. Simultaneous electrochemical/EPR experiments were carried out with an electrolytic flat cell inserted into the EPR cavity. Both the working and the auxiliary electrodes were platinum wires. The surface area of the working electrode inside the EPR cavity was about 1 cm^2. The reference electrode was a silver wire of 75 μm diameter. Electrolysis was controlled by an electrochemical analyzer BAS 100W. The potential applied for bulk electrolysis was 0.1 V more positive than the first oxidation peak. The concentrations of the compounds in CH_2Cl_2 used for electrolysis were (1−2) × 10^{-3} M. After addition of the supporting electrolyte TBAHFP (0.1 M), the samples were purged with Ar (20 min) and then transferred by syringe to the EPR electrolytic cell.

Acknowledgment. This work was supported by grants from the National Science Foundation (CHE-9910177; MPC) and the Division of Chemical Sciences, Office of Basic Energy Sciences of the U.S. Dept. of Energy (DEFG 02-86-ER 13465; L.D.K.). We also thank Dr. Elli Hand for critical reading of the manuscript.

Supporting Information Available: Parameters for the PM3 calculations and magnetic resonance spectra (PMR and CMR). This material is available free of charge via the Internet at http:/pubs.acs.org.

JO010663E